

Chemical studies on antioxidant mechanism of garcinol: analysis of radical reaction products of garcinol and their antitumor activities

Shengmin Sang,^a Min-Hsiung Pan,^b Xiaofang Cheng,^c Naisheng Bai,^a Ruth E. Stark,^c Robert T. Rosen,^a Shoei-Yn Lin-Shiau,^b Jen-Kun Lin^b and Chi-Tang Ho^{a,*}

^aDepartment of Food Science, Center for Advanced Food Technology, Rutgers University, 65 Dudley Road, New Brunswick, NJ 08901-8520, USA

^bInstitute of Biochemistry and Toxicology, College of Medicine, National Taiwan University, 1 Section 1, Jen-ai Road, Taipei, Taiwan, ROC

^cDepartment of Chemistry, College of Staten Island, City University of New York, New York, NY 10314, USA

Received 7 August 2001; accepted 18 September 2001

Abstract—Garcinol (**1**), a polyisoprenylated benzophenone, purified from *Garcinia indica* fruit rind, displays antioxidant properties and is thought to act as an antioxidant in biological systems. However, the mechanisms of its antioxidant reactions remain unknown. The objective of this study was to characterize the reaction products of garcinol with a stable radical, 2,2-diphenyl-1-picrylhydrazyl (DPPH). Structural elucidation of these products can provide insights into specific mechanisms of antioxidant reactions. Two major reaction products, GDPPH-1 (**2**) and GDPPH-2 (**3**), were isolated and identified for the first time. Their structures were determined on the basis of detailed high field 1D and 2D spectral analysis. The identification of these products provides the first unambiguous proof that the principal sites of antioxidant reactions are on the 1,3-diketone and the phenolic ring part of **1**. The induction of apoptosis in human leukemia HL-60 cells, the inhibition of NO generation, the effects on the activity of MMP, and the inhibitory effects on H₂O₂ production of TPA-stimulate HL-60 cells by **1** and its two oxidant products (**2** and **3**) were investigated and would also be discussed in this paper. © 2001 Elsevier Science Ltd. All rights reserved.

1. Introduction

Free radicals and reactive oxygen species play an important physiological role, they are essential for production of energy, synthesis of biologically essential compounds, and phagocytosis, a critical process of immune system.¹ They also play a vital role in signal transduction. On the other hand, there is now increasing evidence that these reactive oxygen species may play a causative role in a variety of diseases including heart disease, aging and cancer.^{2,3} Free radicals and reactive oxygen species attack lipids, sugars, proteins, and DNA and induce their oxidation, which may result in oxidative damage such as membrane dysfunction, protein modification, enzyme inactivation, and breakage of DNA strands and modification of its bases.¹ Consequently, the role of antioxidants has received increased attention during the past decade. It is important to elucidate the mechanisms and dynamics of the oxidative damage in order to understand its biological significance and develop strategies for its prevention. Both active oxygen species and antioxidants are double-edged swords and the balance of their beneficial and toxic effects is determined by the

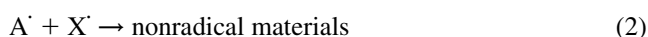
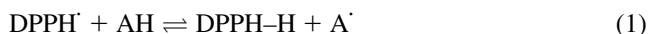
relative importance of many competing biological reactions. Humans have evolved with antioxidant systems to protect against free radicals. These systems include some antioxidants produced in the body (endogenous) and others obtained from the diet (exogenous). Over the past decade, evidence has been accumulated that plant polyphenols are an important class of defense antioxidants. These compounds are widespread virtually in all plant foods, often at high levels, and include phenols, phenolic acids, flavonoids, tannins, and lignans.

Garcinol (**1**) is a polyisoprenylated benzophenone derivative from *Garcinia indica* and other species.^{4–8} The dried rind of *G. indica* (cv. Kokum) which is used as a garnish for curry and in some of the folklore medicine in India contains 2–3% garcinol.^{4,5} Garcinol is structurally similar to a well-known antioxidant-curcumin, which contains both phenolic hydroxyl groups and a β -diketone moiety. Garcinol has been reported to possess antibiotic activities,⁸ antilucer activity,¹⁰ suppressed colonic aberrant crypt foci (ACF) formation,¹¹ and induction of apoptosis through cytochrome c release and activation of caspases in human leukemia HL-60 cells.¹² It also showed strong antioxidant activity. In the H₂O₂–NaOH–DMSO system, garcinol suppressed superoxide anion, hydroxyl radical, and methyl radical; in the Fenton reaction system, garcinol suppressed hydroxyl

Keywords: garcinol; antioxidant mechanism; antitumor activities.

* Corresponding author. Tel.: +1-732-932-9611x235; fax: +1-732-932-6776; e-mail: ho@aesop.rutgers.edu

radical more strongly than DL- α -tocopherol; in the hypoxanthine–xanthine oxidase system, emulsified garcinol suppressed superoxide anion to almost the same extent as DL- α -tocopherol by weight.⁹ It also showed nearly three times greater 2,2-diphenyl-1-picrylhydrazyl (DPPH) free radical scavenging activity than DL- α -tocopherol by weight.¹⁰ However, the antioxidant mechanisms of garcinol remain unclear. To evaluate the antioxidant mechanisms of garcinol, we reacted garcinol with DPPH. The DPPH system is a stable radical-generating procedure.¹³ Because it can accommodate a large number of samples in a short period, and is sensitive enough to detect active principles at low concentrations, it was used in the present study. The antioxidant process of this reaction is thought to be divided into the following two stages:



AH is the antioxidant, A \cdot is the antioxidant radical, and X \cdot is another radical species or the same species as A \cdot .^{1,14} Although the first stage is a reversible process, the second stage is irreversible and must produce stable radical terminated compounds. Structural information about these nonradical products would afford important contributions to the antioxidant mechanism studies.

In this paper, we will report the isolation and structure elucidation of two major oxidation products, GDPPH-1 and GDPPH-2 (**2** and **3**) formed by the reaction of garcinol (**1**) with the stable radical DPPH. The induction of apoptosis in human leukemia HL-60 cells, the inhibition of NO generation, the effects on the activity of MMP, and the

inhibitory effects on H₂O₂ production of TPA-stimulate HL-60 cells by **1** and its two oxidation products (**2** and **3**) have also been evaluated.

2. Results and discussion

2.1. Structural elucidation of two oxidation products (**2** and **3**)

Reaction of garcinol (**1**) with DPPH was carried out and two major oxidation products, GDPPH-1 (**2**) and GDPPH-2 (**3**), were isolated and identified on the basis of their spectral data.

Compound **2**, a yellow amorphous solid, was assigned the molecular formula of C₃₈H₄₈O₆ determined by positive-ion HRFAB-MS ($[\text{M}+\text{H}]^+$ at m/z 601.3527), as well as from its ¹³C NMR data. The molecular formula indicated 15 degrees of unsaturation, which showed that **2** had one more unsaturation than **1**. The ¹H NMR spectrum of **2** showed the presence of two singlets aromatic protons at δ 6.96 and 8.44 ppm, respectively; three isopropylidene groups (three one-hydrogen triplets at δ 5.00, t, $J=6.0$ Hz, 4.76, t, $J=6.0$ Hz, and 4.66, t, $J=6.0$ Hz, and six singlet methyl groups at δ 1.72, 1.64, 1.58, 1.54, 1.44, and 1.09, respectively), one isopropenyl group (two singlets of 2H at δ 4.41 and 4.31, together with a singlet methyl signal at δ 1.56), and two methyl groups on a saturated carbon (two singlets of 3H each at δ 1.29 and 1.22), in addition to methylene and methine protons (a complex multiplet of 12H in the regions of δ 3.00–1.45). Thus the significant difference in the ¹H NMR spectrum of **2** compared to **1** is the loss of one aromatic proton. As we mentioned earlier, **2** had one more

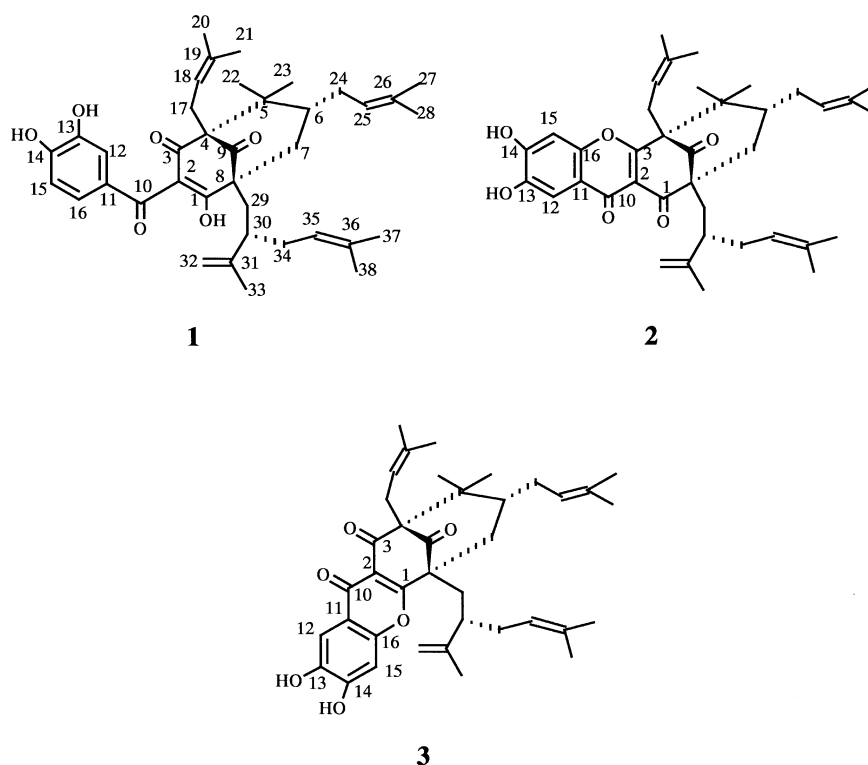


Figure 1. Structures of Garcinol (**1**) and its oxidant products GDPPH-1 (**2**) and GDPPH-2 (**3**).

unsaturation than **1**. All of these mean that there was one more ring in **2** than in **1**. The above findings were in agreement with the ^{13}C NMR spectrum of **2**. It also showed the presence of three isopropylidene groups (three methine carbons of trisubstituted olefinic groups at δ 123.8, 123.0, and 118.8, and six methyl groups at δ 17.9, 18.0, 18.5, 25.9, 26.0, and 26.1), one isopropenyl group (δ 113.9 for a terminal methylene carbon, and δ 18.2 for a methyl signal), and two methyl groups on a saturated carbon (δ 23.5 and 27.4). Two methine carbons for the aromatic ring at δ 102.5 and 110.9; and three oxygen-substituted aromatic carbons at δ 144.7, 150.7, 152.9, which indicated that one aromatic proton of garcinol was substituted by oxygen in **2**. Since both of the aromatic protons in **2** were singlets, it must be H-16 that was substituted by oxygen. Furthermore, in the ^{13}C spectral data, one of the enolized 1,3-diketone in **1** was changed from δ 194.0 (or 195.2) to δ 175.6 in **2**. The ^{13}C spectral data of the carbonyl (C-10) was also changed from δ 199.1 in garcinol to δ 173.1 in **2**. All of these indicated that the oxygen of one of the enolized 1,3-diketone was attached at C-16. The HMBC correlation between $\text{C}_{\delta 175.6}$ and H-17 (δ 2.82 and 2.89), $\text{C}_{\delta 193.4}$ and H-7 (δ 1.99 and 2.44), and H-29 (δ 1.79 and 2.28); $\text{C}_{\delta 173.5}$ and H-12 (δ 8.44), and H-15 (δ 6.96) (Fig. 2) suggested that δ 175.6 was assigned to C-1, δ 193.4 was to C-3, and δ 173.5 was to C-10, respectively. This confirmed that the carbonyl at C-3 was enolized and the oxygen was attached to C-16. Thus, the structure of **2** was deduced as shown (Fig. 1). The complete interpretation of the NMR data was based on the results of COSY, TOCSY, HMQC and HMBC.

Compound **3** was isolated as a yellow amorphous solid. The positive-ion HRFAB-MS of **3** display a molecular ion peak at m/z $[\text{M}+\text{H}]^+$ 601.3527, supporting a molecular formula of $\text{C}_{38}\text{H}_{48}\text{O}_6$, which was the same as the molecular formula of **2**. The ^1H NMR spectrum of **3** displayed a signal pattern similar to that of **2**. It also showed the signals of two singlet aromatic protons at δ 6.91 and 8.38, respectively; three isopropylidene groups (three one-hydrogen triplets at δ 4.97, t, $J=6.0$ Hz, 4.75, t, $J=6.0$ Hz, and 4.64, t, $J=6.0$ Hz, and six singlet methyl groups at δ 1.72, 1.62, 1.56, 1.49, 1.47 and 0.95, respectively), one isopropenyl group (two singlets of 2H at δ 4.11 and 4.14, together with a singlet methyl signal at δ 1.54), and two methyl groups on a saturated carbon (two singlets of 3H each at δ 1.14 and 1.03). The ^{13}C NMR spectrum of **3** also indicated the presence of three isopropylidene groups (three methine carbons of trisubstituted olefinic groups at δ 123.7, 122.5, and 119.7, and six methyl groups at δ 17.7, 18.1, 18.5, 22.6,

25.8, and 25.9), one isopropenyl group (δ 112.2 ppm for a terminal methylene carbon, and δ 18.3 for a methyl signal), and two methyl groups on a saturated carbon (δ 27.3 and 29.9), two methine carbons for the aromatic ring at δ 102.5 and 110.6; and three oxygen-substituted aromatic carbons at δ 144.6, 150.2, 152.8. The data of $\text{C}_1\text{--C}_3$ (δ 114.5, 178.2, and 193.5) and C_{10} (δ 173.7) were also similar with those of **2**. All of these indicated that **3** was an isomer of **2**. This was confirmed by the cross peaks in the HMBC spectrum. In the HMBC of **3**, the correlations between $\text{C}_{\delta 193.5}$ and H-17 (δ 2.59 and 2.71), $\text{C}_{\delta 178.2}$ and H-7 (δ 2.15 and 2.38), and H-29 (2.01 and 2.24); $\text{C}_{\delta 173.5}$ and H-12 (δ 8.38), and H-15 (δ 6.91) (Fig. 2) suggested that δ 178.2 was assigned to C-1, δ 193.5 was to C-3, and δ 173.7 was to C-10, respectively. Thus, the structure of **3** was identified as shown (Fig. 1). For compound **2** the carbonyl at C-3 was enolized and the oxygen was attached to C-16, while for compound **3** the carbonyl at C-1 was enolized and the oxygen was attached to C-16. The complete interpretation of the NMR data was based on the results of COSY, TOCSY, HMQC and HMBC.

2.2. Induction of apoptosis by garcinol (1), GDPPH-1 (2), and GDPPH-2 (3) in human leukemia HL-60 cells

A sub-G1 (sub-2N) DNA peak, which has been suggested to be the apoptotic DNA was detected in cells that were treated with **1–3**, washed, and stained with propidium iodide. As shown in Fig. 3, the percentage of apoptotic HL-60 cells were 9.85, 66.34, and 66.33% after 12 h of incubation with **1–3** (10 μM), respectively. Among them, **2** appeared to be more potent, with an EC_{50} of 8.4 μM and induced dose-dependent on the cell apoptosis. When the cells were treated with the same concentration (20 μM) of compounds, the apoptotic potency was the same. These data are consistent with DNA fragmentation.

2.3. Inhibition of NO generation by garcinol (1), GDPPH-1 (2), and GDPPH-2 (3)

Compounds **1–3** were examined to determine whether they affect NO production in macrophages activated with LPS for 24 h. Of these compounds tested, **1** inhibited LPS-stimulated NO generation the most strongly; however, **1–3** all markedly reduced NO generation in a concentration-dependent manner (Fig. 4). At concentrations of 2.5, 5, and 10 μM , **1** inhibited NO generation by 49, 87, and 92%, respectively. At concentrations of 2.5, 5, and 10 μM , **2** inhibited NO generation by 45, 75, and 78%, respectively. At concentrations of 2.5, 5, and 10 μM , **3** inhibited NO

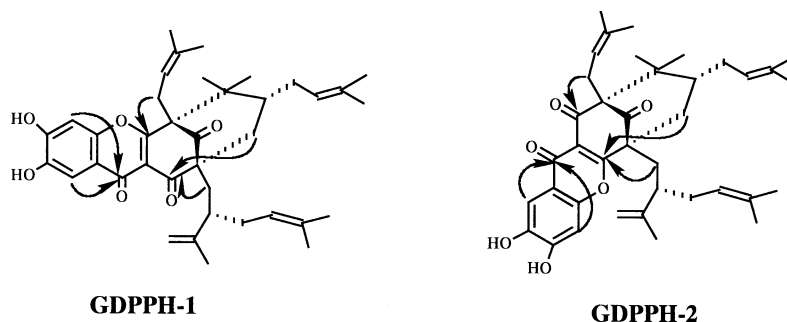


Figure 2. Significant HMBC (H→C) correlations of GDPPH-1 (2) and GDPPH-2 (3).

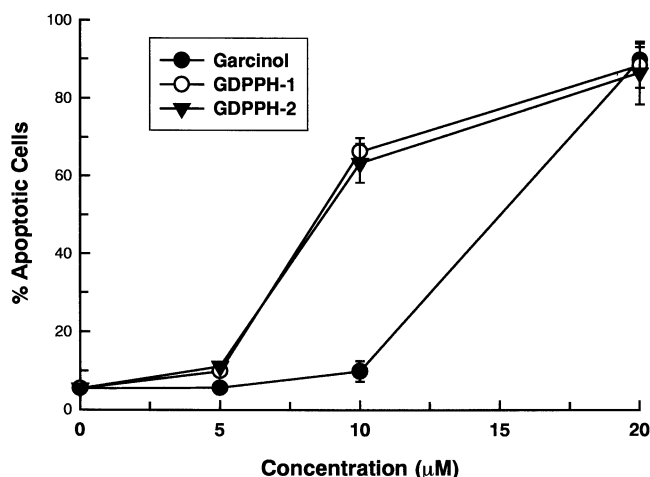


Figure 3. Inducing apoptosis of HL-60 cells by compounds 1–3 (garcinol, GDPPH-1, and GDPPH-2). Cells were harvested 12 h after treatment, and apoptosis was quantified by flow cytometry. The method of flow cytometry used is described under Experimental.

generation by 19, 62, and 73%, respectively. Inhibition of NO production was not due to cytotoxicity, as determined with the trypan blue exclusion assay.

2.4. Effects of garcinol (1), GDPPH-1 (2), and GDPPH-2 (3) on the activity of MMP

MMPs expression has been correlated with metastatic potential. We determined the effects of 1–3 on the activity of MMP by zymographic analysis. The same number of cells were seeded, and the MMP activity of conditioned medium from the cells were measured with three compounds for 24 h. As shown in Fig. 5, the inhibitory potency was estimated in the following order: 1>3>2 at 2 μM. The inhibition of MMP activity was not due to toxicity, as determined by trypan blue exclusion assay.

2.5. Effects of garcinol (1), GDPPH-1 (2), and GDPPH-2 (3) on H₂O₂ production of TPA-stimulated HL-60 cells

Studies of the effects of 1–3 on H₂O₂ production by TPA-stimulate HL-60 cells were analyzed by flow cytometry. The results show that garcinol was the most potent inhibitor of TPA-induced H₂O₂ production in HL-60 cells at 5 μM (Fig. 6). The inhibitory potency was estimated in the following order: 1>3>2 at 5 μM. The effects of 1–3 on H₂O₂ production in TPA-stimulated HL-60 cells are possibly involved in the signal transduction of the PKC activation pathway that is stimulated by TPA.

2.6. Discussions

Two compounds (2 and 3) were isolated from the radical reaction products of garcinol (1) and DPPH. From our elucidation of the chemical structures of these two

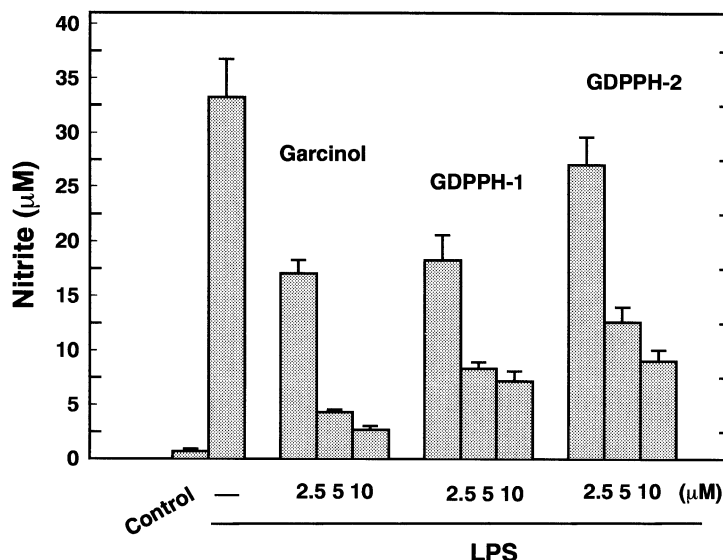


Figure 4. Effects of compounds 1–3 (garcinol, GDPPH-1, and GDPPH-2) on LPS-induced nitrite production in RAW 264.7 Cells. The cells were treated with different concentrations of compounds and LPS (100 μg mL⁻¹) for 24 h. Nitrite were determined by Griess reaction, as described in Experimental. The values were expressed as means±SE of triplicate tests.

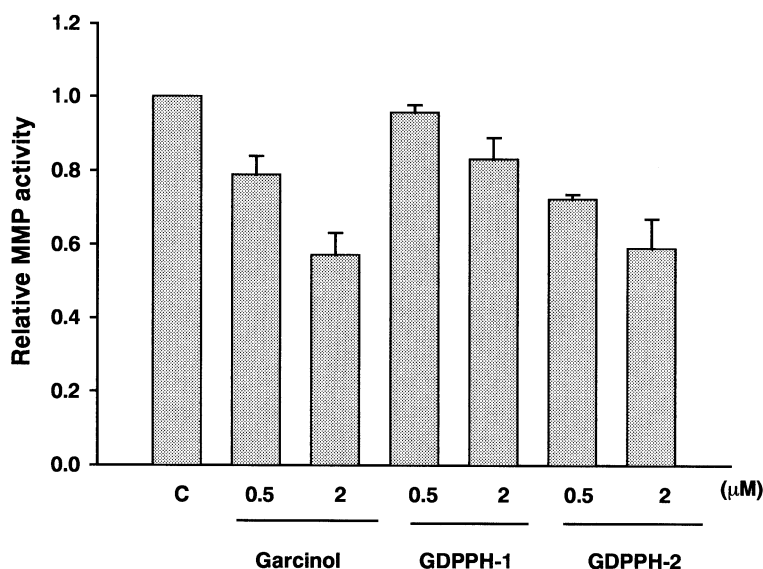


Figure 5. Gelatin-based zymography (MMP activity) of the culture medium of B16 cells. B16 cells were treated with various concentrations of compounds 1–3 (garcinol, GDPPH-1, and GDPPH-2) for 24 h, and MMP activity of culture medium were determined by zymographic assay. The values were expressed as means \pm SE of triplicate tests.

compounds, we proposed the antioxidant mechanism of garcinol as illustrated in Fig. 7. As shown in Fig. 7, garcinol donated an H atom from the hydroxyl group of the enolized 1,3-diketone to form a pair of resonance. If the H atom of the hydroxyl group at C-3 was donated, **2** would be formed, and **3** was given when the H atom of the hydroxyl group at C-1 was trapped by the DPPH radical.

The antitumor test of garcinol and its two reaction products (GDPPH-1 and GDPPH-2) on the induction of apoptosis in human leukemia HL-60 cells, the inhibition of NO generation, the effects on the activity of MMP, and the

inhibitory effects on H_2O_2 production of TPA-stimulate HL-60 cells indicated that like **1**, both **2** and **3** showed inhibitory effects on these assay. More importantly, **2** appeared to be more potent than **1**, with an EC_{50} of $8.4 \mu M$ and induced dose-dependent on the cell apoptosis. The potency of these compounds in apoptosis-induction may vary with the different cell lines. These findings might suggest possible chemopreventive ability of garcinol and its two oxidation products. Thus, analysis of these products could prove a unique tool for assessing the contribution of antioxidant reactions to the disease preventive effects of garcinol.

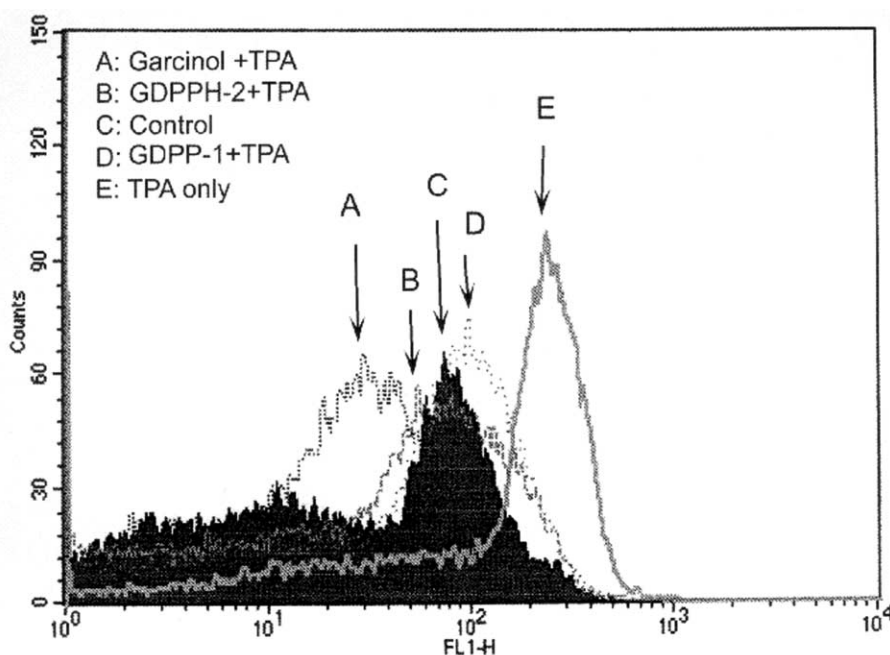


Figure 6. Inhibition of TPA-stimulated H_2O_2 production in HL-60 cells. Studies of the effects of compounds 1–3 (garcinol, GDPPH-1, and GDPPH-2) on H_2O_2 production by TPA-stimulated HL-60 cells were performed as described in the Experimental.

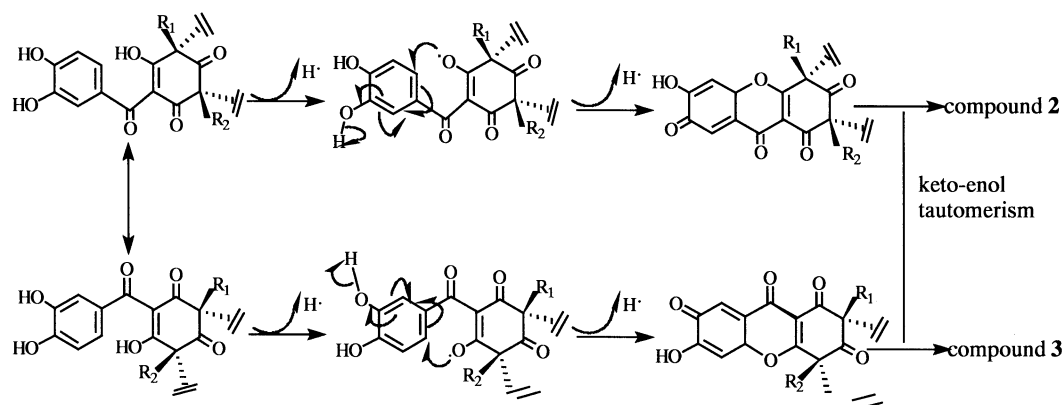


Figure 7. Proposed mechanism for the formation of oxidation product GDPPH-1 (2) and GDPPH-2 (3).

Our future work will focus on whether reaction products of garcinol and free radicals in lipid bilayers in vitro and in biological membranes in vitro and in vivo are similar to those observed in this study in a homogeneous solution system. We are also very interested in the studies that it is garcinol or its oxidation products or both of them that play the functional role in the biological systems.

3. Experimental

3.1. General procedures

^1H (600 MHz), ^{13}C (150 MHz) and all 2D NMR spectra were run on Varian AM-600 NMR spectrometer, with TMS as internal standard. FT-IR was performed on a Magna 550 spectrometer. HRFAB-MS was run on JEOL HX-110 double focusing mass spectrometer. The APCI MS was performed on a Fisons/VG Platform II mass spectrometer. Thin layer chromatography was performed on Sigma–Aldrich TLC plates (250 μm thickness, 2–25 μm particle size), with compounds visualized by spraying with 5% (v/v) H_2SO_4 in ethanol solution. DPPH was purchased from Sigma Chemical Co. CD_3OD was purchased from Aldrich Chemical Co.

3.2. Preparation of garcinol

Garcinol was prepared from *G. indica* dried fruit rind that was extracted with ethanol. The extract was subjected to silica gel column eluted with hexane–ethyl acetate solvent system.¹⁵ The fractions containing garcinol were concentrated and dried in vacuo. The residue was dissolved in hexane, and remained in the freezer for 24 h to get yellow amorphous powder from the solution and washed with cold hexane on a glass filter. After recrystallization, the powder was dissolved in hot acetonitrile at room temperature; pale yellow crystal needles were obtained from the solvent. The crystals were identified as garcinol (4,7) from the following spectral data: ^1H NMR (CDCl_3): 6.93 (1H, dd, $J=7.8$, 2.0 Hz), 6.91 (1H, d, $J=2.0$ Hz), 6.60 (1H, d, $J=7.8$ Hz), 4.92, 5.02, 5.06 (1H each, t, $J=6.0$ Hz), 4.38, 4.34 (1H each, s), 2.80–1.46 (12H, m, methylene and methine), 1.77, 1.71, 1.67, 1.63, 1.57, 1.52, 1.50, 1.14, 0.98 (3H each, s); ^{13}C NMR (CDCl_3): Table 1; Positive APCI-MS: m/z 603 $[\text{M}+\text{H}]^+$.

Table 1. δ_{H} (600 MHz) NMR spectral data of compounds 2, 3 and δ_{C} (150 MHz) NMR spectral data of compounds 1–3 (CD_3OD) (δ in ppm, J in Hz)

	1, δ_{C}		2		3	
	δ_{C}	δ_{H}	δ_{C}	δ_{H}	δ_{C}	δ_{H}
1	194.0 s	193.4 s			178.2 s	
2	116.0 s	119.8 s			114.5 s	
3	195.2 s	175.6 s			193.5 s	
4	69.9 s	64.0 s			71.7 s	
5	49.8 s	49.9 s			50.1 s	
6	47.0 d	46.8 d	1.45 m		46.3 d	1.50 m
7	42.7 t	43.2 t	1.99 m		42.3 t	2.15 m
			2.24 m			2.38 m
8	58.1 s	62.0 s			55.6 s	
9	207.1 s	207.9 s			207.5 s	
10	199.1 s	173.5 s			173.7 s	
11	127.8 s	117.7 s			114.5 s	
12	114.4 d	110.9 d	8.44 s		110.6 d	8.38 s
13	143.9 s	150.7 s			150.2 s	
14	149.9 s	152.9 s			152.8 s	
15	116.6 d	102.5 d	6.96 s		102.5 d	6.91 s
16	120.2 d	144.7 s			144.6 s	
17	27.2 t	26.0 t	2.82 dd, 6.6, 14.4		26.1 t	2.59 dd, 6.6, 14.4
			2.89 dd, 6.6, 14.4			2.71 dd, 6.6, 14.4
18	122.8 d	118.8 d	4.76 t, 6.0		119.7 d	4.75 t, 6.0
19	135.5 s	135.3 s			134.9 s	
20	26.2 q	26.1 q	1.58 s		26.2 q	1.56 s
21	18.4 q	18.5 q	1.72 s		18.5 q	1.72 s
22	22.9 q	23.5 q	1.29 s		22.6 q	1.14 s
23	27.2 q	27.4 q	1.22 s		27.3 q	1.03 s
24	29.1 t	29.5 t	1.69 m		29.9 t	1.60 m
			1.93 m			1.96 m
25	123.9 d	123.8 d	4.66 t, 6.0		123.7 d	4.64 t, 6.0
26	133.1 s	133.2 s			133.1 s	
27	25.9 q	25.9 q	1.44 s		25.8 q	1.47 s
28	18.1 q	17.9 q	1.09 s		17.7 q	0.95 s
29	36.3 t	37.6 t	1.79 m		36.4 t	2.01 m
			2.28 m			2.24 m
30	43.7 d	43.9 d	2.74 m		44.2 d	2.38 m
31	148.2 s	149.2 s			147.2 s	
32	112.9 t	113.9 t	4.31 s		112.2 t	4.11 s
			4.41 s			4.14 s
33	17.8 q	18.2 q	1.56 s		18.3 q	1.54 s
34	32.8 t	32.4 t	1.97 m		33.2 t	2.00 m
			2.00 m			2.16 m
35	124.2 d	123.0 d	5.00 t, 6.0		122.5 d	4.97 t, 6.0
36	132.2 s	132.9 s			132.5 s	
37	26.0 q	26.0 q	1.64 s		25.9 q	1.62 s
38	18.1 q	18.0 q	1.54 s		18.1 q	1.49 s

3.3. Oxidation of 1 and isolation of reaction products 2 and 3

Garcinol (**1**) (1.0 g, 1.67 mmol) was allowed to react with DPPH (1.3 g, 3.34 mmol) in acetone at room temperature under darkness for 24 h. After evaporation of the solvent in vacuo, the residue was first applied to silica gel column eluting with chloroform first to get rid of the DPPH and **1** (60 mg) and then with chloroform–acetone (10:1) to get a mixture of two reaction products. The mixture of two reaction products was subjected to RP-C18 silica gel column eluting by 90% methanol–water solvent system to give 90 mg compound **2** and 30 mg compound **3**.

Compound **2** was isolated as a pale amorphous substance: IR (film) ν_{\max} : 3300, 2918, 2849, 1732, 1681, 1616, 1512, 1465, 1390, 1293, 1190, 1143 cm^{-1} ; ^1H NMR (CD_3OD , 600 MHz): see Table 1; ^{13}C NMR (CD_3OD , 150 MHz): see Table 1; positive HRFAB-MS m/z 601.3527 $[\text{M}+\text{H}]^+$ (calcd for $\text{C}_{38}\text{H}_{49}\text{O}_6$, 601.3529).

Compound **3** was isolated as a pale amorphous substance: IR (film) ν_{\max} : 3300, 2910, 2845, 1725, 1680, 1615, 1510, 1465, 1390, 1285, 1140 cm^{-1} ; ^1H NMR (CD_3OD , 600 MHz): see Table 1; ^{13}C NMR (CD_3OD , 150 MHz): see Table 1; positive HRFAB-MS m/z 601.3527 $[\text{M}+\text{H}]^+$ (calcd for $\text{C}_{38}\text{H}_{49}\text{O}_6$, 601.3529).

3.4. Cell culture and chemicals

Human promyelocytic leukemia (HL-60) cells obtained from American Type Culture Collection (Rockville, MD) were grown in 90% RPMI 1640 and 10% fetal bovine serum (GIBCO BRL, Grand Island, NY), supplemented with 2 mM glutamine (GIBCO BRL), 1% penicillin–streptomycin (10,000 units of penicillin/mL and 10 mg mL^{-1} streptomycin). RAW 264.7 cells were cultured in RPMI-1640 (without phenol red) supplement with 10% endotoxin-free heat-inactivated fetal calf serum (GIBCO, Grand Island, NY). Mouse B16 melanoma cells were maintained in Dulbecco's modified Eagle's medium (DMEM) containing 10% heat-inactivated fetal bovine serum. Lipopolysaccharide (LPS) (*Escherichia coli* 0127: B8), 12-*O*-tetradecanoylphorbol-13-acetate (TPA), and propidium iodide were purchased from Sigma (St Louis, MO). 2',7'-Dichlorofluorescein diacetate (DCF-DA) was purchased from (Molecular Probes, Eugene, Oregon, USA).

3.5. Flow cytometry

HL-60 cells (2×10^5) were cultured in 60 mm Petri dishes and incubated for 12 h. Then cells were harvested, washed with PBS, resuspended in 200 μL of PBS, and fixed in 800 μL of iced 100% ethanol at -20°C . After being left to stand overnight, the cell pellets were collected by centrifugation, resuspended in 1 mL of hypotonic buffer (0.5% Triton X-100 in PBS and 0.5 $\mu\text{g mL}^{-1}$ RNase), and incubated at 37°C for 30 min. Then 1 mL of propidium iodide solution (50 $\mu\text{g mL}^{-1}$) was added, and the mixture was allowed to stand on ice for 30 min. Fluorescence emitted from the propidium iodide–DNA complex was quantitated after excitation of the fluorescent dye by FACScan cytometry (Becton Dickinson, San Jose, CA).

3.6. DNA extraction and electrophoresis analysis

HL-60 cells (5×10^5 cells/mL) were harvested, washed with PBS, and then lysed with digestion buffer containing 0.5% sarkosyl, 0.5% mg mL^{-1} proteinase K, 50 mM tris(hydroxymethyl)aminomethane (pH 8.0), and 10 mM EDTA at 56°C for 3 h and treated with RNase A (0.5 $\mu\text{g mL}^{-1}$) for another 2 h at 56°C . The DNA was extracted by phenol–chloroform–isoamyl (25:24:1) before loading and analyzed by 1.8% agarose gel electrophoresis. The agarose gels were run at 50 V for 120 min in Tris–borate/EDTA electrophoresis buffer (TBE). Approximately 20 μg of DNA was loaded in each well and visualized under UV light and photographed.

3.7. Nitrite assay

The nitrite concentration in the culture medium was measured as an indicator of NO production, according to the Griess reaction. One hundred microliters of each supernatant was mixed with the same volume of Griess reagent (1% sulfanilamide in 5% phosphoric acid and 0.1% naphthylethylenediamine dihydrochloride in water). Absorbance of the mixture at 550 nm was determined with an enzyme-linked immunosorbent assay plate reader (Dynatech MR-7000; Dynatech Labs, Chantilly, VA).

3.8. Zymographic assay for metalloproteinase

The amount of gelatinase in the conditioned media (serum free) was estimated and quantified by cell numbers. Conditioned media were concentrated, and then equal amounts, based on cell numbers determined at the time of harvest, were electrophoresed in 10% SDS-PAGE containing 0.1% (w/w) gelatin. The gel was washed twice, each time for 30 min at room temperature in solution containing 2.5% (v/v) Triton X-100, and subsequently transferred to a substrate buffer containing 10 mM CaCl_2 , and 500 mM Tris–HCl, pH 8.0, at 37°C with shaking for 18 h. Finally, the gel was stained for 1 h with 0.25% (w/v) Coomassie blue in 10% acetic acid (v/v) and 50% methanol and the destained in 8% acetic acid and 5% methanol (v/v).

3.9. Determination of hydrogen peroxide by DCF-DA in the flow cytometer

DCFH-DA is a nonfluorescent probe, which becomes fluorescent in the presence of hydrogen peroxide. This dye is stable nonpolar compound that readily diffuses into the cells and is hydrolyzed by intracellular esterase to yield dichlorodihydrofluorescein (DCFH), which is trapped within the cell. Hydrogen peroxide or low molecular weight peroxides, produced during oxidative respiratory burst, oxidize DCFH to highly fluorescent 2',7'-dichlorofluorescein (DCF). HL-60 (1×10^6) cells were stimulated with the addition of 100 ng mL^{-1} TPA and the desired concentration of tested compounds at 37°C for 30 min. The cells were treated with 30 μM for a further 30 min and suspended in PBS and were analyzed in the FACScan laser flow cytometry (Becton Dickinson, San Jose, CA).

References

1. Papas, A. M. *Antioxidant Status, Diet, Nutrition, and Health*; CRC: Florida, USA, 1999 pp 3–20.
2. Slater, T. *Biochem. J.* **1984**, *222*, 1–15.
3. Yagi, K. *Chem. Phys. Lipids* **1987**, *45*, 337–351.
4. Krishnamurthy, N.; Lewis, Y. S.; Ravindranath, B. *Tetrahedron Lett.* **1981**, *22*, 793–796.
5. Krishnamurthy, N.; Ravindranath, B. *Tetrahedron Lett.* **1982**, *23*, 2233–2236.
6. Bakana, P.; Claeys, M.; Totte, J.; Pieters, L. A. C.; Van Hoof, L.; Van Den Berghe, D. A.; Vlie-Tink, A. J. *J. Ethnopharmacol.* **1987**, *21*, 75–84.
7. Sahu, A.; Das, B.; Chatterjee, A. *Phytochemistry* **1989**, *28*, 1233–1235.
8. Iinuma, M.; Tosa, H.; Tanaka, T.; Kanamaru, S.; Asai, F.; Kobayashi, Y.; Miyauchi, K.; Shimano, R. *Biol. Pharm. Bull.* **1996**, *19*, 311–314.
9. Yamaguchi, F.; Ariga, T.; Yoshimura, Y.; Nakazawa, H. *J. Agric. Food Chem.* **2000**, *48*, 180–185.
10. Yamaguchi, F.; Saito, M.; Ariga, T.; Yoshimura, Y.; Nakazawa, H. *J. Agric. Food Chem.* **2000**, *48*, 2320–2325.
11. Tanaka, T.; Kohno, H.; Shimada, R.; Kagami, S.; Yamaguchi, F.; Kataoka, S.; Ariga, T.; Murakami, A.; Koshimizu, K.; Ohigashi, H. *Carcinogenesis* **2000**, *21*, 1183–1189.
12. Pan, M. H.; Chang, W. L.; Lin-Shiau, S. Y.; Ho, C. T.; Lin, J. K. *J. Agric. Food Chem.* **2001**, *49*, 1464–1474.
13. Deby, C.; Magotteau, G. *CR Soc. Biol.* **1970**, *164*, 267–268.
14. Frankel, E. N. *Lipid Oxidation*; The Oily Press: Dundee, Scotland, 1998 pp 129–160.
15. Still, W. C.; Kahn, M.; Mitra, A. *J. Org. Chem.* **1978**, *43*, 2923–2925.